Journal of New Materials for Electrochemical Systems 12, 153-159 (2009)

Successive Loadings of Reactant in the Hydrogen Generation by Hydrolysis of Sodium Borohydride in Batch Reactors

M. J. F. Ferreira[1], V. R. Fernandes[2], C. M. Rangel[3], L. Gales[4] and A. M. F. R. Pinto[*,5]

[1]INEGI - Instituto de Engenharia Mecânica e Gestão Industrial, Rua Dr. Roberto Frias 378, 4200-465 Porto, Portugal
[2]INETI - Unidade de Electroquímica de Materiais, Estrada do Paço do Lumiar, 1649-038 Lisboa, Portugal
[3]Laboratório Nacional de Energia e Geologia- LNEG/ Fuel Cells and Hydrogen, Estrada do Paço do Lumiar, 1649-038 Lisboa, Portugal
[4]IBMC - Instituto de Biologia Molecular e Celular, Universidade do Porto, Rua do Campo Alegre 823, 4150-180 Porto & ICBAS - Instituto de Ciências Biomédicas Abel Salazar, Largo Prof. Abel Salazar 2, 4099-003 Porto, Portugal
[5]CEFT - Centro de Estudos de Fenómenos de Transporte, Departamento de Engenharia Química, Faculdade de Engenharia da Universidade do Porto, Rua Dr. Roberto Frias s/n, 4200-465 Porto, Portugal

Received: April 2, 2009 , Accepted: June 6, 2009

***Abstract**: In this paper, for the first time, an experimental investigation is presented of five successive loadings of reactant alkaline solution of sodium borohydride ($NaBH_4$) for hydrogen generation, using an improved nickel-based powder catalyst, under uncontrolled ambient conditions. The experiments were performed in two batch reactors with internal volumes of 0.646 l and of 0.369 l. The compressed hydrogen generated, at pressures below hydrogen critical pressure, gives emphasis on the importance of considering solubility effects during reaction, leading to storage of hydrogen in the liquid phase inside the reactor. The present work suggests that the sodium metaborate by-product formed by the alkaline hydrolysis of $NaBH_4$, in a closed pressure vessel without temperature control, is $NaBO_2.xH_2O$, with $x \geq 2$.*

The data obtained in this work lends credit to $x \approx 2$, which was discussed based on the XRD results, and this call for increased caution in the definition of the hydrolysis reaction of $NaBH_4$ up to temperatures of 333 K and up to pressures of 0.13 MPa.

Keywords: Sodium borohydride; nickel-based catalyst; hydrogen generation; hydrogen storage; high pressure; fuel cell

1. INTRODUCTION

The advent of low or carbon-free primary energy sources are of unprecedented interest for a sustainable world's energy economy. In this context, hydrogen is being labelled the energy carrier after the 'petroleum era'. As a combustible fuel, hydrogen produces more energy per kg (12.24×10^4 kJ) than fossil coal, petroleum and natural gas. In addition, hydrogen, as a fuel, has a number of advantages including: minimal environmental pollution; mass transportability comparable to petroleum and natural gas; combustibility in internal combustion engines (Carnot-cycle devices) and rocket engines; and feasibility of electrochemical combination with an oxidant in fuel cells [1].

Proton exchange membrane fuel cells (PEMFC) have been intensively studied in the last decade. This free-energy device is a 'factory' that takes H_2 and O_2 as input and produces electricity as output. Pure hydrogen is required as the fuel in PEMFC and among many known vials of obtained it and storage it [2], precursor chemicals play an important role in hydrogen based energy systems, for example various types of hydrides including the chemical hydrides.

Among the chemical hydrides, sodium borohydride ($NaBH_4$) has a number of advantages over all other hydrides. It is a compound of known composition which can be made to liberate a stoichiometric amount of hydrogen, is stable under ordinary storage conditions and does not undergo violent reaction [1]. Schlesinger et al. [3] recognized the potential usefulness of $NaBH_4$ as a hydrogen generator, and the particularly striking catalytic effect of certain transition metals and their salts on its hydrolysis rate. Relevant work was carried out during sixties [1, 4-5], and more recently Amendola [6,7] gave a practical, controlled and portable concept of molecular hydrogen generation using catalytic

*To whom correspondence should be addressed: Email: apinto@fe.up.pt
Tel.: +351 22 508 1675; Fax: +351 22 5081449

aqueous sodium borohydride solutions.

$NaBH_4$ reacts with water to generate molecular hydrogen according to the hydrolysis reaction shown in Eq.(1):

$$NaBH_4 + (2+x)\ H_2O \rightarrow NaBO_2.xH_2O + 4\ H_2 + \text{heat}. \quad (1)$$

Ideal hydrolysis is attained for $x = 0$ [3], but in practice excess of water is required accounting for the fact that the solid by-product can exist with varying degrees of hydration [8-10]. A direct consequence of this is the value of hydrogen storage density. In fact, hydrogen storage capacity can be as high as 21 wt% based on the amount of hydrogen generated per unit mass of sodium borohydride consumed, but the real formation of the hydrated by-product severely compromises the overall storage density, which can be calculated to be close to 4.2 wt% by taking the amount of hydrogen produced divided by the total weight of the reactants [11].

At room temperature, sodium borohydride reacts slowly with water according to Eq.(1), but the reaction can be enhanced by rising the medium temperature, by addition of acids or catalysts [1,3]. Lyttle et al. [12] observed that commercial borohydride deteriorates rapidly in aqueous solution, but is fairly stable in basic solutions and furthermore the higher the pH the greater the stability. This finding brought the solution pH as the limiting parameter of (1) and forced researchers to find a practical and controlled way of producing hydrogen by the use of catalysts. Heterogeneous catalysis offers a number of advantages: independence of solution pH over a wide range, controllable hydrolysis rate and the reuse of the catalyst.

There has been much research performed on the hydrogen generation using catalysts. Several metal catalysts are effective reaction catalysts to enhance hydrolysis of the alkaline sodium borohydride solution. Among them, the catalysts with precious metals most used are: rhodium, platinum, ruthenium [5-7], platinum supported on $LiCoO_2$, CoO and TiO_2 [13-15] or carbon [16], ruthenium supported on IRA-400 anion resin [17] or alumina pellets [18], ruthenium nanoclusters [19], and Pt/Pd on carbon nanotubes (CNT) paper [20]. The most used high-performance catalyst containing non-noble metals are: nickel [3, 21], nickel and/or cobalt borides [1, 4, 22-29], cobalt boride supported on nickel foam [30, 31] or carbon [32], cobalt boride amorphous alloy powder and Pd/C [33], cobalt on γ -alumina [34], hydrogenphosphate-stabilized nickel(0) nanoclusters [35], Co-Mn-B supported on nickel foam [36], and Co-P catalyst [37,38]. A metal alloy catalyst containing a less precious metal: $Ru_{60}Co_{20}Fe_{20}$ supported on activated carbon fibber, have been reported by Park *et al.* [39], who found high hydrogen release in the reaction given by Eq.(1).

Excluding the works of Kojima [15] and Pinto [25], all the works mentioned in the previous paragraph reported experiments performed in reaction vessels at ambient pressure. In a previous paper, a nickel-based catalyst was found to work as a good catalyst for releasing hydrogen by hydrolysis of $NaBH_4$ solution in a batch reactor [25]. The catalyst produced less than the expected 100% conversion of the theoretical amount of hydrogen using different concentrations of alkali in excess of water. This result was related with solubility effects, in which the solubility of hydrogen was greatly enhanced by the rising of pressure during the reaction, leading to H_2 storage in the liquid phase. In this paper, it is shown for the first time, an experimental investigation of successive loadings of alkaline sodium borohydride ($NaBH_4$) solution for hydrogen generation, using an improved nickel-based powdered catalyst, under uncontrolled ambient conditions. The system produced high H_2 pressure and can be generated in large amounts sufficient for use in a low power PEMFC single cell and stack.

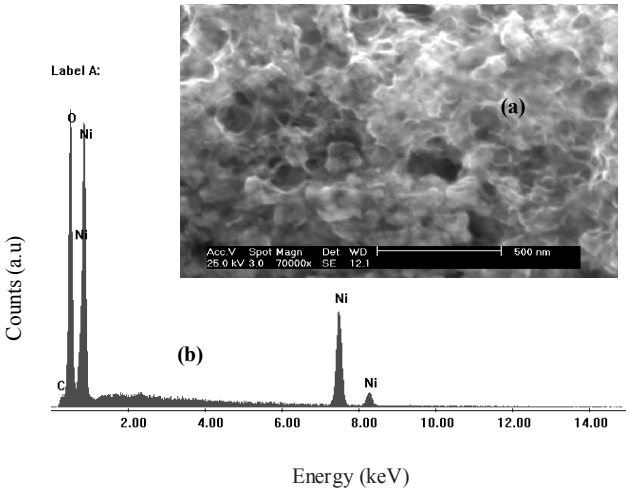

Figure 1. Scanning electron microscope view of the synthesized catalyst powder (a) and associated elemental analysis EDAX (b).

2. EXPERIMENTAL

2.1. Catalyst preparation

A nickel-based catalyst in the form of a finely divided powder was prepared from a mixture of precursors based on nickel salts (Riedel-de Haën) by chemical reaction with 10 wt% borohydride solution (Rohm and Haas), as the reducing environment. The catalyst, characterized by a large specific surface area, was appropriately decanted, washed, filtered, dried and heat-treated at 110 ºC. The catalyst was kept in a dessicator until use. In this work, the catalyst is used in powder form, unsupported. Catalyst samples were analyzed for morphology and elemental analysis on a Phillips Scanning Electron Microscope, Model XL 30 FEG, coupled to EDAX. Figure 1 shows morphology of the powder exhibiting nanometric particle size and elemental analysis showing nickel as a main constituent.

2.2. Hydrogen generation

2.2.1. Chemicals

Sodium borohydride powder (96% purity) and sodium hydroxide powder (98% purity) were supplied by MERCK (No.: 1.06371.0100) and by EKA (No.: 1310.73.2) respectively, and were used as received. Deionised water was used to prepare all the aqueous solutions. The $NaBH_4$ concentration tested was 10 wt%, and for the inhibitor we used NaOH concentration of 1 wt%, 7 wt% and 10 wt%. In all the stabilized solutions the pH was 14. For the catalyst used in the present work, a proportion of Ni-based/NaBH4: 0.4 g/g was found suitable.

2.2.2. Experimental rig and procedure

Figure 2 shows a picture of the sodium borohydride generation

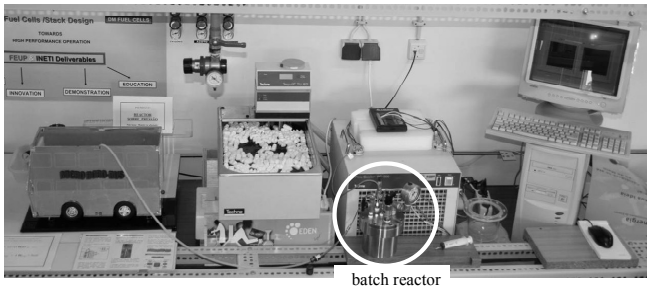

Figure 2. General view of the experimental rig, highlighting the batch reactor.

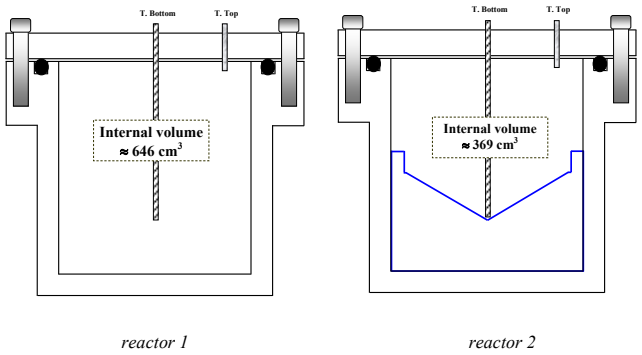

Figure 3. Schematic view of the inside of the reactors: *reactor 1* – plane bottom, and *reactor 2* – conical bottom.

system. The specific details of experimental procedures are explained on an earlier work [25].

Two major improvements were made in the reactor design which allowed an axial installation of O-ring for reactor sealing and the possibility of following the reaction temperature using two k thermocouples positioned at two distinct points inside the reactor: one near its bottom (named T.Bottom) and the other one very close to its top (named T.Top). Figure 3 shows the exposed view of the news reactors.

The two reactors used in the experiments have an internal free volume of 646 cm^3 and of 369 cm^3, the last one with an inside conical bottom geometry. This configuration enables nondispersible effects of contacting powdered catalyst with the reactant injected solution. Experimental tests were performed without magnetic stirring and without temperature control. A proper quantity of nickel-based powdered catalyst was previously measured in an analytical balance and then stored in the bottom of the reactor. After the reactor being perfectly sealed, an adequate amount of reacting solution was rapidly injected into the reactor with a syringe with a very high needle length (150 mm) to ensure that the reacting solution is delivered very close to the catalyst. The temperature of the reactor medium was monitored and recorded simultaneously with a data acquisition system using Labview software. To monitor the rate of hydrogen generation, the gas pressure inside the reactor was followed with an appropriate pressure probe.

Figure 4. Crystals of sodium metaborate (*dehydrated*), obtained by slow evaporation of water solution at room temperature (≈25 ºC).

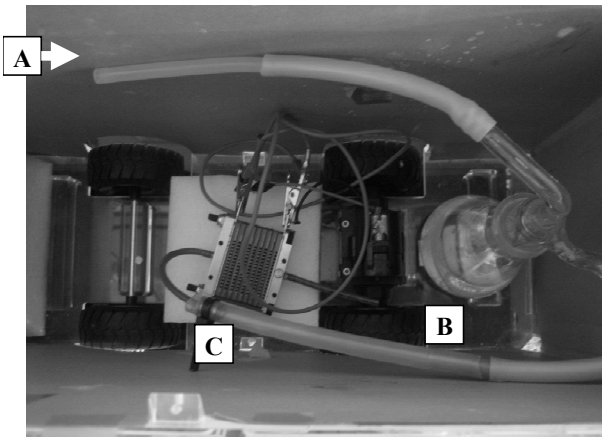

Figure 5. Top view of the "MicroBoro Bus": A – connection to the H_2 generator and storage tank; B- gas-washing bottle; C- PEMFC single cell.

2.3. By-product analysis

The by-product of the hydrogen generation reactions after five successive loadings was analyzed with X-Ray Diffractometry (XRD). Suitable crystals – see Figure 4, were obtained by slow evaporation of water solution and were orthorhombic, space group *Pca21*, cell volume V=364.62(4) Å3. Unit cell parameters a = 10.7252(7) Å, b = 5.2525(3) Å, c = 6.4724(4) Å, α= β = γ = 90º (uncertainties in parentheses). There are four molecules per unit cell, calculated density 2.237 g/cm^3. Diffraction data were collected at 293 K with a Gemini PX Ultra equipped with MoKα radiation (λ=0.71073 Å). A total of 562 independent reflections were measured, of which 501 were observed (I>2σ (I)). The structure was solved by direct methods using SHELXS-97 [40] with atomic positions and displacement parameters refined with SHELXL-97 [41]. The non-hydrogen atoms were refined anisotropically and the hydrogen atoms were refined freely with isotropic displacement parameters. The refinement converged to R(all data) = 3.93% and $wR2$(all data) = 9.92%.

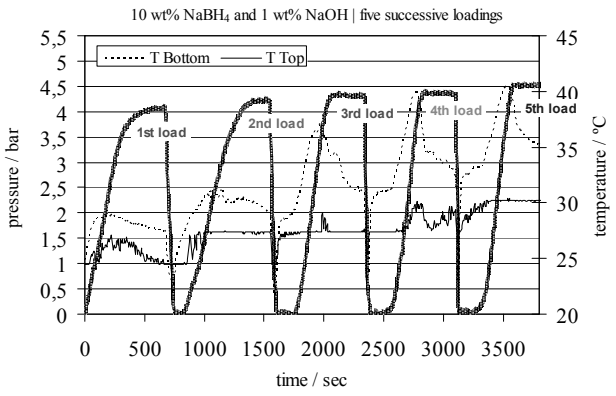

Figure 6. Five successive loadings of the reactant solution: 10 wt.% $NaBH_4$, 1 wt.% NaOH, 89 wt.% H_2O, with Ni-based/$NaBH_4$: 0.4g/g, performed in the batch *reactor 1*, showing the temperature profile inside the reactor at two specific points.

2.4. Connecting to PEMFC single cell

The hydrogen generated by successive loadings of reactant solutions was supplied to a PEMFC single cell that was housed in a bus like shape mobile platform, used for didactic proposes – the "MicroBoro Bus" [26]. Figure 5 shows the top view of that didactic prototype. The single cell was fed with *pure* hydrogen generated by catalytic hydrolysis of $NaBH_4$, loading after loading, and the *purity* of the molecular gas was simply checked by measurements of the initial and final pH of the liquid water inside the gas-washing bottle. No significant variance in pH value was found.

3. RESULTS AND DISCUSSION

3.1. Hydrogen generation

In this paper, following recent published works by the authors [25, 26], an experimental investigation is for the first time presented of successive loadings of alkaline $NaBH_4$ solution of 10 wt.% $NaBH_4$ with different amounts of NaOH, specifically 1, 7 and 10 percent by weight. Powder reused nickel-based catalyst performs very well the hydrolysis reaction given by equation (1). A proportion of Ni-based/$NaBH_4$: 0.4g/g was found appropriate and was used in all the experiments.

The hydrogen yield in reaction (1) was calculated assuming 100% conversion of $NaBH_4$ by applying the ideal gas law to the final volume of gas inside the reactor, with x=2. Special care was taken to correct the free varying volume of gas inside the reactor between each successive reactant loadings.

Figure 6 shows the behaviour of five successive loadings of reactant solution in the batch reactor 1, with concentration of 10 wt% $NaBH_4$, 1 wt.% NaOH, 89 wt.% H_2O. It was found suitable to show the importance of the variation of temperature inside the reactor that occurs during one fuel single loading. Similar trends were detected in the experiments performed in the batch reactor 2.

As can be seen in the plot of Fig.6, the rising of temperature at the bottom of the reactor (T.Bottom) occurs during each individual fuel loading until reaches the "plateau", and this effect is more pronounced in the lasts loadings. When the temperature is not controlled, the exothermic characteristics of reaction (1) give rise to

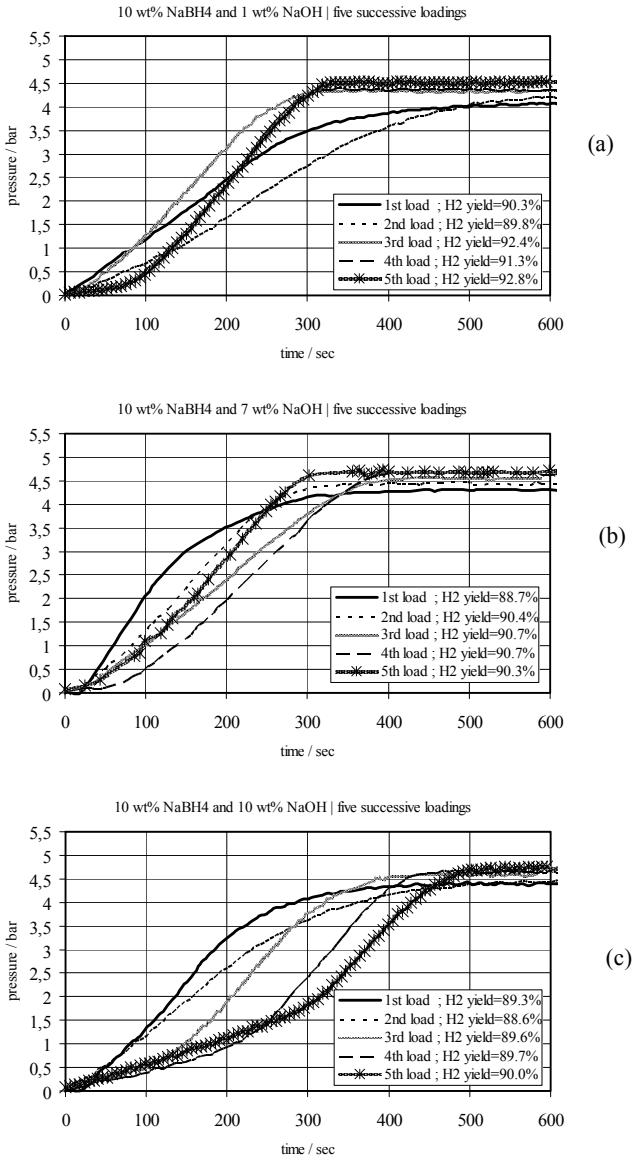

Figure 7. Hydrogen generation in batch *reactor 1* of five successive loadings of the reactant solution, with Ni-based/$NaBH_4$: 0.4g/g: (a) 10 wt.% $NaBH_4$, 1 wt.% NaOH, 89 wt.% H_2O, (b) 10 wt.% $NaBH_4$, 7 wt.% NaOH, 83 wt.% H_2O and (c) 10 wt.% $NaBH_4$, 10 wt.% NaOH, 80 wt.% H_2O.

the medium gas temperature near the top of the reactor (positioned vertically, see Fig.3). This is favourable, due to the hydrolysis kinetics, because it leads to an increase of H_2 pressure with smaller amount of the needed activation energy required by the (same quantity of) catalyst, which is housed in the bottom of the reactor.

The fluctuations detected in the reactor temperature along reaction (see Fig.6), also indicate at which rates the hydrogen is being generated, i.e., a smooth pattern of the internal reactor temperature profile, both at the bottom and at its top, indicates a slowly hydrolysis kinetics; but, an asymptotically and random patterns in reactor temperature profiles, put in evidence the dynamic behaviour

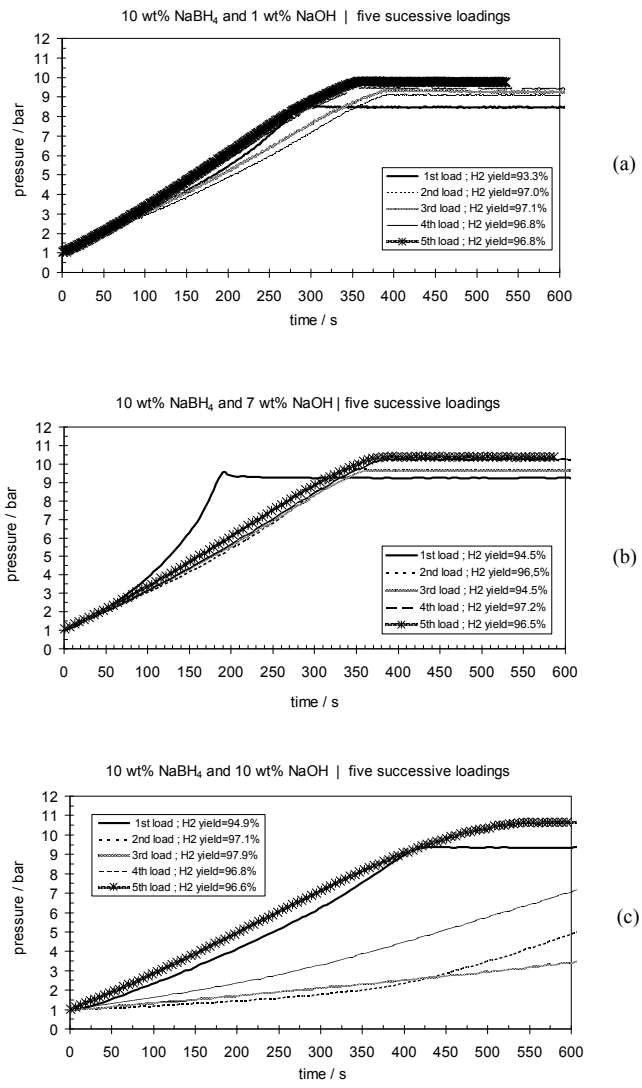

Figure 8. Hydrogen generation in batch *reactor 2* of five successive loadings of the reactant solution, with Ni-based/$NaBH_4$: 0.4g/g: (a) 10 wt.% $NaBH_4$, 1 wt.% NaOH, 89 wt.% H_2O, (b) 10 wt.% $NaBH_4$, 7 wt.% NaOH, 83 wt.% H_2O and (c) 10 wt.% $NaBH_4$, 10 wt.% NaOH, 80 wt.% H_2O.

of reactants and products inside the reactor due to increased internal pressure. The plots in Fig. 7 corroborates with this observations, showing a higher hydrogen yield for the 3rd and 5th loadings in both of which the variation of temperature were more pronounced.

Plots in Figure 7 - 8 shows a typical course of a hydrogen generation reaction presented in terms of the operating pressure as a function of time, for five successive loadings of *fuel* solution, respectively, in batch reactor 1 and 2. These results show an improvement in the performance of the recent Ni-based catalyst, comparing with the similar trend published by Pinto [25], the latter with a larger particle size. In fact, this nano-powdered Ni-based catalyst gives high H_2 yield in a relatively short reaction time until the 'plateau' is achieved. It is worth mentioning the tendency of the

Figure 9. "Gaseous" by-product effect after five successive loadings. The H_2 release shows the gas capability to agitate the nickel-based powdered catalyst presented at the reactor liquid phase.

catalyst to perform better, with a higher H_2 yield, after the first loading of reactant (the amount of catalyst remains the same from the first to the last loading). A possible explanation for a lower yield in the first loading could be the higher capability of the liquid phase to store hydrogen by solubility effects, which tend to decrease for the subsequent loadings. This may be very important if we think on the solubility of hydrogen enhanced by the rising pressure during reaction. As mention by Pinto [25], the increasing pressure of the gas phase inside the reactor, due to hydrogen generation, forces at the same time, the hydrogen dissolution. This is an interesting finding since molecular hydrogen was generated but also stored in the liquid phase.

Figure 9 shows the gaseous by-product effect obtained after a quick exit from the reactor at the end of the reaction of five successive loadings, preceded by the released of H_2 to the atmosphere. As we can see, the "sparkling" by-product quickly dissipates the H_2 bubbles along the glass, showing the gas capability to agitate the nickel-based powdered catalyst presented at the reactor liquid phase. This proves that a significant amount of the H_2 generated inside the reactor was trapped in the liquid reactor phase, keeping it dissolved, and was after release just due to pressure difference.

In Tables 1-3 we can see the performance of the same reactions in the two reactors tested. Apparently, the reaction rate is enhanced by lower values of NaOH concentration and by a succession of loadings of fuel.

The average yield of H_2 generation is higher in the reactor with a smaller internal volume (reactor 2) for the same concentration of liquid reactant solution. One possible explanation for this fact could be the bottom geometry – conical configuration, which might improve the contact of the powder catalyst with the injected reactant solution. Another possible explanation could be the increase in the activity of the nickel boride catalyst under high pressure (the pressure in the reactor 2 is higher than in the reactor 1), probably owing to synergistic effects. A similar trend was found by Kojima [15] with a noble Pt-$LiCoO_2$ catalyst under a ratio catalyst/$NaBH_4$: 0.5g/g.

Table 1. Five successive loadings of reactant solution: 10 wt% $NaBH_4$ and 1 wt% NaOH.

1 wt% NaOH	*reactor 1* (plane bottom)	*rector 2* (conical bottom)
Internal volume (cm^3)	646	369
H_2 average yield (%)	91	98
Reaction time (min.)	5-5.8	4.8-5.8

Table 2. Five successive loadings of reactant solution: 10 wt% $NaBH_4$ and 7 wt% NaOH.

7 wt% NaOH	*reactor 1* (plane bottom)	*rector 2* (conical bottom)
Internal volume (cm^3)	646	369
H_2 average yield (%)	90	96
Reaction time (min.)	5.5-6.5	3.5-6.5

Table 3. Five successive loadings of reactant solution: 10 wt% $NaBH_4$ and 10 wt% NaOH.

10 wt% NaOH	*reactor 1* (plane bottom)	*rector 2* (conical bottom)
Internal volume (cm^3)	646	369
H_2 average yield (%)	89	97
Reaction time (min.)	7.5-8.5	7-11

3.2. Reaction by-product characterization

The crystal structure of reaction (1) by-product after five successive loadings of reactant solution reveals that the boron atoms are in a triangular configuration with three oxygen atoms, with B-O bond lengths between 1.27 and 1.29 Å. The BO_3 triangular arrangement was already found in the crystal structure of orthorhombic [42] and monoclinic [43] metaboric acid, although in the title crystal structure the oxygen atoms are bound to just one B atom. The BO_3 triangles form layers 3.238 Å apart that sandwich a layer of sodium and water molecules (see Fig. 10). For each boron atom there are three bound oxygen atoms and one water oxygen. Half of the sodium atoms have their valence strength distributed between six Na-O bonds and the other half between seven Na-O bonds (as already determined in other sodium metaborate structures [44]). The water molecules are involved in a net of interactions with the sodium atoms (see Fig. 10).

We found that the reaction (1) by-product after five successive loadings of reactant solution is a sodium metaborate dehydrated. Thus, the reaction of successive loadings of $NaBH_4$ on stabilized solutions using the same amount of Ni-based catalyst under high pressure is shown as follows

$$NaBH_4 + 4\ H_2O \rightarrow NaBO_2.2H_2O + 4\ H_2 + \text{heat}. \quad (2)$$

4. CONCLUSIONS

In this paper a new experimental investigation using successive loadings of reactant solution in a batch reactor for H_2 generation by catalytic hydrolysis of sodium borohydride was developed. Experiments, performed in two closed pressure vessel, without controlled reaction temperature, put in evidence the molar relation $H_2O/NaBH_4$=4, and the large quantities of H_2 generated proves the good performance of the nickel-based catalyst used. The activity of the catalyst seems to increase under high pressure after successive loadings.

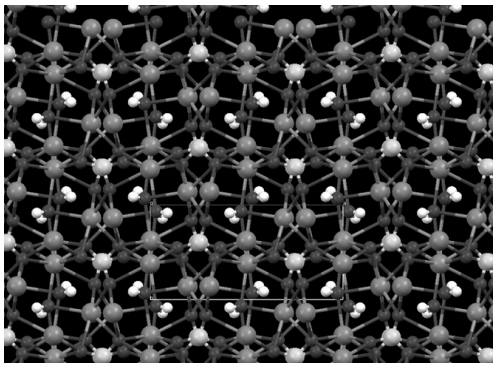

Figure 10. View along the *c*-axis of the crystal structure of sodium metaborate dehydrate, showing the BO_3 triangular arrangement and the Na bound network. Na in violet, O in red, B in pink and H in white.

The increase of the dynamic behaviour of reactants and products inside the reactor by the rise of the internal pressure probably enhance the solubility of hydrogen in the liquid phase even in the absence of mechanical stirring. The temperature profiles during the reaction time, loadings after loadings, put in evidence this assumption.

The capability of re-use a constant amount of catalyst during successive loadings of *fuel*, without any treatment and without loss of activity, is a major finding if we having in mind the possible applications of this concept for hydrogen generation and storage.

5. ACKNOWLEDGEMENTS

This research was performed under the scope of the EDEN Project (http://www.h2eden.com), Task PR07.33.01 - *Hydrogen generation via chemical hydrides*, funded by the Agência de Inovação SA of Portugal (http://www.adi.pt).

L. Gales acknowledges the financial support from FCT-Portugal (Project PTDC/CTM/64191/2006).

REFERENCES

[1] C. M. Kaufman, B. Sen, J. Chem. Soc. Dalton Trans., 307 (1985).

[2] L. Schlapbach, A. Züttel, Nature, 414, 353 (2001).

[3] H. I. Schlesinger, H. C. Brown, A.E . Finholt, J. R. Gilbreath, H. R. Hoekstra, E. K. Hyde, J. Am. Chem. Soc., 75, 215 (1953).

[4] A. Levy, J. B. Brown, C. J. Lyons, Industrial Engng. Chemistry, 52, 211 (1960).

[5] H. C. Brown, C. A. Brown, J. Am. Chem. Soc., 84, 1493 (1962).

[6] S. C. Amendola, S. L. Sharp-Goldman, M. S. Janjua, N. C. Spencer, M. T. Kelly, P. J. Petillo, M. Binder, Int. J. Hydrogen Energy, 25, 969 (2000).

[7] S. C. Amendola, S. L.Sharp-Goldman, M. S. Janjua, M. T. Kelly, P. J. Petillo, M. Binder, J. Power Sources, 85, 186 (2000).
[8] W. C. Blasdale, C. M. Slansky, J. Am. Chem. Soc., 61, 917 (1939).
[9] E. Y. Marreo-Alfonso, J. R. Gray, T. A. Davis, M. A. Matthews, Int. J. Hydrogen Energy, 32, 4717 (2007).
[10]E. Y. Marreo-Alfonso, J. R. Gray, T. A. Davis, M. A. Matthews, Int. J. Hydrogen Energy, 32, 4723 (2007).
[11]C.-T. F. Lo, K. Karan, B. R. Davis, Ind. Eng. Chem. Res., 46, 5478 (2007).
[12]D. A. Lyttle, E. H. Jensen, W. A. Struck, Analytical Chemistry, 24, 1843 (1952).
[13]Y. Kojima, K.-I. Suzuki, K. Fukumoto, M. Sasaki, T. Yamamoto, Y. Kawai, H. Hayashi, Int. J. Hydrogen Energy, 27, 1029 (2002).
[14]Y. Kojima, K.-I Suzuki, K. Fukumoto, Y. Kawai, M. Kimbara, H. Nakanishi, S. Matsumoto, J. Power Sources, 125, 22 (2004).
[15]Y. Kojima, Y. Kawai, H. Nakanishi, S. Matsumoto, J. Power Sources, 135, 36 (2004).
[16]C. Wu, H. Zhang, B. Yi, Catalysis Today, 477, 93 (2004).
[17]P. Krishnan, T.-H. Yang, W.-Y. Lee, C.-S. Kim, J. Power Sources, 143, 17 (2005).
[18]J. S. Zhang, W. N. Delgass, T. S. Fisher, J. P. Gore, J. Power Sources, 164, 772 (2007).
[19]S.Özkar, M. Zahmakiran, J. Alloys and Compounds, 728, 404 (2005).
[20]R. Peña-Alonso, A. Sicurelli, E. Callone, G. Carturan, R. Raj, J. Power Sources, 165, 315 (2007).
[21]J.-H. Kim, K.-T. Kim, Y.-M. Kang, H.-S. Kim, M.-S. Song, Y.-J. Lee, P.S. Lee, J.-Y. Lee, J. Alloys and Compounds, 379, 222 (2004).
[22]D. Hua, Y. Hanxi, A. Xinping, C. Chuansin, Int. J. Hydrogen Energy, 28, 1095 (2003).
[23]S. U. Jeong, R. K. Kim, E. A. Cho, H.-J. Kim, S.-W. Nam, I.-H. Oh, S.-A. Hong, S. H. Kim, J. Power Sources, 144, 129 (2005).
[24]B. H. Liu, Z. P. Li, S. Suda, J. Alloys and Compounds, 415, 288 (2006).
[25]A. M. F. R. Pinto, D. S. Falcão, R. A. Silva, C. M. Rangel, Int. J. Hydrogen Energy, 31, 1341 (2006).
[26]C. M. Rangel, R. A. Silva, A. M. F. R. Pinto *in* "Proceedings of the International Conference in Power Engineering and Electric Drives", Eds. L.S. Martins and P. Santos, Setúbal, Portugal, September 12-14, 2007, paper 237.
[27]J. C. Ingersoll, N. Mani, J. C. Thenmozhiyal, A. Muthaiah, J. Power Sources, 173, 450 (2007).
[28]S. U. Jeong, E. A. Cho, S. W. Nam, I. H. Oh, U. H. Jung, S. H. Kim, Int. J. Hydrogen Energy, 32, 1749 (2007).
[29]J. C. Walter, A. Zurawski, D. Mongomery, M. Thornburg, S. Revankar, J. Power Sources, 179, 335 (2008).
[30]S. J. Kim, J. Lee, K. Y. Kong, C. R. Jung, I.-G. Min, S.-Y. Lee, H.-J. Kim, S. W. Nam, T.-H. Lim, J. Power Sources, 170, 412 (2007).
[31]J. Lee, K. Y. Kong, C. R. Jung, E. Cho, S. P. Yoon, J. Han, T.-G. Lee, S. W. Nam, Catalysis Today, 120, 305 (2007).
[32]J. Zhao, H. Ma, J. Chen, J. Hydrogen Energy, 32, 4711 (2007).
[33]C. Zanchetta, B. Patton, G. Guella, A. Miotello, Meas. Sci. Technol., 18, N21 (2007).
[34]W. Ye, H. Zhang, D. Xu, L. Ma, B. Yi, J. Power Sources, 164, 544 (2007).
[35]Ö. Metin, S. Özkar, Int. J. Hydrogen Energy, 32, 1707 (2007).
[36]M. Mitov, R. Rashkov, N. Atanassov, A. Zielonka, J. Mater. Sci., 42, 3367 (2007).
[37]K. W. Cho, H. S. Kwon, Catalysis Today, 120, 298 (2007).
[38]K. Eom, K. W. Cho, H. S. Kwon, J. Power Sources, 180, 484 (2008).
[39]J. H. Park, P. Shakkthivel, H. J. Kim, M. K. Han, J. H. Jang, Y. R. Kim, H. S. Kim, Y. G. Shu, Int. J. Hydrogen Energy, 33, 1845 (2008).
[40]Sheldrick, G. M. SHELXS-97, Program for the solution of crystal structures; University of Göttingen: Germany 1997.
[41]Sheldrick,G. M. SHELXL-97, Program for the refinement of crystal structures; University of Göttingen: Germany 1997.
[42]H. Tazaki, J. Sci. Hiroshima Univ A, 10, 37, 55 (1940).
[43]W. H. Zachariasen, Acta Cryst., 16, 385 (1963).
[44]M. Marezio, H. A. Plettinger, W. H. Zachariasen, Acta Cryst., 16, 594 (1963).